GeoVirtual 2020 September 14-16 Resilience and Innovation

# Reliability Assessment of Drag Embedment Anchors in Layered Seabed, Clay over Sand

Amin Aslkhalili & Hodjat Shiri
*Civil Engineering Department, Memorial University of Newfoundland, St. John's, NL, Canada*

ABSTRACT
Reliability assessment of drag embedment anchors are required to have a safe exploration and production of offshore reserves. The currently used anchor design codes consider only homogeneous seabed soil conditions, and layered seabed condition effects have not been investigated. In this study, the reliability of anchors was comprehensively investigated in the clay over sand seabed. An advanced calculation tool was developed to obtain the holding capacity of the anchors. Time-domain dynamic mooring analysis was conducted by assuming a semi-submersible platform to capture the dynamic line tensions. The uncertainties of the environmental loads, metocean variables, seabed soil properties were incorporated into a FORM to obtain the failure probabilities. The study revealed a significant effect of the layered soil condition in reliability assessment by lowering the magnitude of reliability indexes and the necessity of incorporation of the complex seabed conditions into design codes to have a safer and cost-effective anchor design.

RÉSUMÉ
L'évaluation de la fiabilité R des ancres d'intégration de traînée est exigée pour avoir une exploration et la production sûres des réserves extracôtières. Les codes de conception d'ancre actuellement utilisés ne considèrent que l'état homogène du sol des fonds marins, et les effets de l'état des fonds marins en couches n'ont pas été étudiés non plus. Dans cette étude, la fiabilité des ancres a été étudiée de manière exhaustive dans l'argile sur le fond marin dessable. Un outil de calcul avancé a été mis au point pour obtenir la capacité de détention des ancres. Temps-analyse dynamique d'amarrage de domaine a été menée en assumant une plate-forme semi-sous-solsible pour obtenir les tensions dynamiques de ligne. Les incertitudes des charges environnementales, des variables métacraines, des propriétés du sol des fonds marins ont été incorporées dans un FORM pour obtenir les probabilités de défaillance. L'étude a révélé un effet significatif de l'état du sol en couches dans l'évaluation de la fiabilité en abaissant l'ampleur des indices de fiabilité et la nécessité d'intégrer les conditions complexes des fonds marins dans les codes de conception pour avoir une conception d'ancrage plus sûre et rentable.

## 1 Introduction

Catenary mooring systems along with their seabed anchors are often used to keep a wide range of offshore floating facilities such as operating vessels, semi-submersibles, spars, floating production storage and offloading (FPSOs) stationary, etc. Different types of anchors are in a mooring system such as suction anchors, pile anchors, screw-in anchors, plate anchors, deadweight anchors, and drag embedment anchors. However, the latter one is amongst the most popular seabed anchoring solutions that are used for both temporary and permanent mooring systems. Temporary mooring systems are usually used with construction vessels and floating exploration units. These systems are retrieved at the end of the operation. The permanent mooring systems are used for floating production facilities and remain in the seabed for the operating lifespan of the unit (Figure 1).

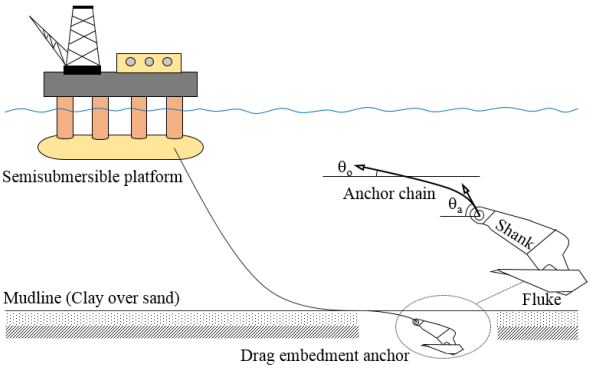


Figure 1. Drag embedment anchor configuration with a catenary mooring line

The operational and environmental safety of the floating facilities significantly depends on the reliability of mooring and anchoring systems. Expanding the offshore explorations and operations towards the deep waters and harsh environments has resulted in developing high capacity anchoring and mooring solutions with high-strength components. However, the number of mooring system related incidents in harsh environments involving floating facilities (on an average of more than two incidents per year reported by Duggal et al. 2013) continue to raise concerns in the industry in general. On the other hand, large uncertainties in seabed parameters and environmental loads combined with the inaccessibility for monitoring, inspection, and maintenance mandates the reliability assessment of drag anchors to minimize their likelihood of failure.

It becomes more challenging when the seabed soil strata comprise layered conditions such as clay over sand, sand over clay, sand over sand, etc., since depending on the anchor trajectory in the layered soil, the ultimate holding capacity may significantly vary (O'Neill et al. 1997). In layered seabed conditions, the existing design codes recommend the same capacity assessment procedure as homogeneous soil. This simplification may affect the reliability of the drag anchors and impose some level of risk to the project. This important aspect has never been studied in the past and needs investigations to facilitate refining the design code recommendations for layered soil.

The reliability of some of the anchor families such as suction caissons have been widely investigated in the literature (Clukey et al., 2013; Choi, 2007; Valle-molina et al., 2008; Silva-González et al., 2013; Montes-Iturrizaga and Heredia-Zavoni, 2016; Rendón-Conde and Heredia-Zavoni, 2016). However, there are only two studies (to the best of the authors' knowledge) on the reliability of drag embedment anchors (Moharrami and Shiri, 2018; Aslkhalili et al., 2019) both of which have considered a single homogeneous layer of clay and sand, respectively.

In this study, the influence of layered seabed on reliability and the likelihood of failure of drag embedment anchors supporting the catenary mooring lines were comprehensively investigated. Clay over sand stratum was considered, which is commonly found in offshore territories. A generic semi-submersible platform in the Flemish Pass Basin, Newfoundland Offshore (East Canada) was simulated by fully coupled time-domain analyses to obtain the dynamic tensions of mooring lines. The response surface method was employed for conducting probabilistic model of the line tensions at the mudline. The probabilistic modeling of anchor capacity was conducted using a limit state equilibrium and kinematic approach to characterize the fluke-soil interaction and failure states. The embedded profile and the frictional capacity of the anchor chain at the seabed were also considered in the calculation of ultimate holding capacity. The uncertainties of the environmental loads, metocean variables, and consequently, the stress distribution throughout the catenary lines were accounted for using the response surface method. First order reliability method (FORM) was used through an iterative procedure to obtain the probabilistic failures.

## 2 Methodology

The reliability study was conducted based on a limit state function assessing the anchor holding capacity against the dynamic mooring line tensions at mudline. The anchor response in the layered soil (clay over sand), along with the soil-chain interaction was obtained by adopting the limit state equilibrium and kinematic approach and the procedure proposed by O'Neill et al. (1997). An Excel spreadsheet VBA Macro (Visual Basic Application) was programmed to calculate the holding capacity of anchor incorporating the effect of the soil-chain interaction. In order to obtain the mean and maximum dynamic line tensions, mooring analysis was conducted using OrcaFelx by assuming a generic semi-submersible platform in the Flemish Pass Basin, NL offshore (Canada), and the sea states with a 100 years return period.

Stevpris Mk5 and Mk6 anchors were considered for reliability studies with the key parameters including undrained shear strength, effective clay unit weight, fluke and shank bearing factor, clay and sand boundary layer depth, effective sand unit weight, sand friction angle, dilation angle, anchor geometrical configurations, line tension angle at mudline, and side friction factor. Response surface method was used to function the mean and predicted maximum of dynamic line tension using uncertain metocean variables. The reliability analysis was conducted by using the first order reliability method (FORM). The required data related to partial design factors for capacities and the mean and maximum dynamic line tensions were obtained from DNV-RP-E301 (2012).

## 3 Modeling Drag Anchor in Layered Soil

### 3.1 Anchor holding capacity

The holding capacity of drag embedment anchor in layered soil (clay over sand) was obtained by combining the limit equilibrium and kinematic solutions for homogeneous clay and sand layers (O'Neill 2000). Four main episodes were defined to cover three different domains of clay-only, sand-only, and clay over sand seabed:

The anchor is entirely in the clay layer and has not yet entered the sand.

The anchor fluke tips have just passed the sand-clay interface.

The anchor fluke has fully or significantly embedded in the sand layer, but all or part of the shank is still in the clay layer.

The anchor fluke and shank are entirely embedded in the sand layer beneath the clay.

The first episode was adopted from Neubecker and Randolph (1996b) with no modification. The episode was identified by incremental checking of the fluke tip depth, $d_t$, which needed to be less than the clay layer depth, $d_c$. When the fluke tip passes the clay-sand interface ($d_t > d_c$), the second episode starts. In this episode, the clay-only domain is still dominant, but the effect of the fluke tip encountered with the sand layer was considered. O'Neill (2000) proposed the following equation for calculation of fluke tip force that was added to $T_a$ to obtain the revised anchor capacity, $T_a'$:

$$F_t = A_t q_{sand} N_t \quad [1]$$

where $A_t$ is the projected area of fluke tips on a perpendicular plane to moving direction, $q_{sand}$ is the standard sand strength, and $N_t$ is bearing factor of fluke tip in the sand. The direction of $F_t$ assumed to be parallel to the direction of movement.

The standard sand strength, $q_{sand}$, was obtained by:

$$q_{sand} = \gamma_c' d_c + \gamma_s' (d_t - d_c) \quad [2]$$

As the anchor embeds further in the seabed, it reaches a point which the dominant mechanism changes to sand. The exact position of transition point is not well known; nevertheless, O'Neill (2000) proposed, as the bottom depth of front shank face, $d_{sf}$, transcends depth of clay-sand interface, $d_c$, the governing mechanism changes to sand-dominant behavior. Modifications were done to the sand-dominant mechanism to use in this episode: first, adding the normal and shear forces of clay on the fluke and shank, second, incorporating the clay overburden pressure. Figure 2 shows the modified acting forces on a drag anchor which has the sand-dominant mechanism.

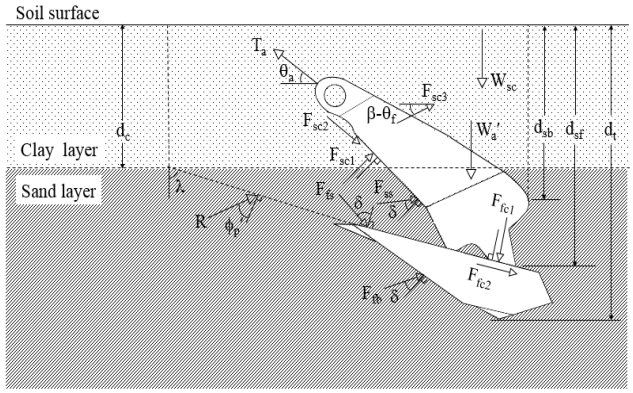


Figure 2. Force system of anchor-soil in clay over sand

As indicated in Figure 2, the clay normal and shear fluke force, $F_{fc1}$ and, $F_{fc2}$, are perpendicular and parallel to the top fluke face and they could exist when shank front depth and shank back depth be respectively, greater and less than clay depth layer ($d_{sf} \geq d_c$, $d_{sb} < d_c$). The clay normal, $F_{sc1}$, and shear, $F_{sc2}$, act normal and oriented to the front shank face, and they exist when pad-eye depth is less than clay layer depth ($d_a < d_c$). The clay side shank force, $F_{sc3}$, acts parallel to moving direction. The weight of soil wedge, $W_{sc}$, side friction, SF, and, the sand shank force, $F_{ss}$, need to be modified compared to sand only force system and the updated functions used in calculations. The modified formulations of all these forces can be found in O'Neill (2000).

The fourth episode is achieved by deep penetration of the anchor, where the fluke and shank are completely embedded within the sand layer. The calculation procedure for this episode is the same as the third episode by two corrections. First, the fluke and shank clay forces become zero; second, the influence of sand layer is considered for determination of the inclination angle at the attachment point of chain and pad-eye.

The force-free body diagram of the anchor in clay over sand layered soil was determined by using the mentioned four episodes and their relevant modified forces. The unknown parameters are soil resistance, R, sand fluke force, $F_{fs}$, the force behind the flukes, $F_{fb}$, and the chain tension, and $T_a$ which was calculated by using soil failure wedge, the anchor force free-body diagram, and applying vertical and horizontal force equilibriums.

It is worth mentioning; the ultimate holding capacity is sensitive to the anchor geometry idealization approach that is used in an analytical solution. In this study, the idealization method proposed by Neubecker and Randolph (1996b) was adopted. Aslkhalili et al. (2019) have discussed the influence of anchor geometry idealization impact on its holding capacity and consequently, the reliability indexes.

The anchor embedment trajectory in the layered soil (clay over sand) was obtained by using the methodology proposed by Neubecker and Randolph (1996a) and extended by O'Neill et al. (1997). The adopted methodology has been developed based on a minimum work approach. The anchor, at some point in the soil with ultimate forces acting on it needs a certain amount of work to be translated and rotated to some new geometry in the soil. A series of assumed displacements and rotations are automatically tried to obtain the incremental relocation dissipating the least amount of work. The corresponding displacement increment with the least dissipated energy is assumed to be the anchor trajectory with the least resistance against the anchor relocation. More details of the proposed kinematic model for the layered soil (clay over sand) could be found in Neubecker and Randolph (1996a) and O'Neill (2000).

### 3.2 Developing Calculation Spreadsheet

The ultimate holding capacity and the trajectory of the anchor-chain system was calculated by developing an Excel spreadsheet equipped with VBA macros for iterative calculations. The performance of the developed spreadsheet was verified against the published experimental and analytical studies O'Neill (2000). The anchor, chain, and layered soil input parameters for the validation study are summarized in Table 1.

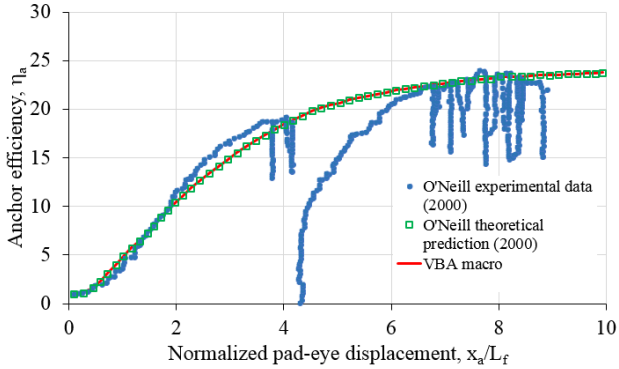


Figure 3. Evaluation of developed spreadsheet with O'Neill studies

Table 1. Soil and anchor input parameters in the current analysis

| Parameter | Value |
|---|---|
| Anchor dry weight, $W_a$ (kN) | 313.6 |
| Fluke length, $L_f$ (m) | 4.97 |
| Fluke width, $b_f$ (m) | 4.23 |
| Fluke thickness, $d_f$ (m) | 0.72 |
| Shank length, $L_s$ (m) | 8.07 |
| Shank width, $b_s$ (m) | 0.83 |
| Fluke-Shank angle, $\theta_{fs}$ (°) | 27.1 |
| Effective chain width, $b_c$ (m) | 0.24 |
| Chain self-weight, $w_c$ (kN/m) | 2 |
| Chain soil friction coefficient $\mu$ | 0.4 |
| Peak friction angle, $\phi_p$ (°) | 35 |
| Shank bearing factor, $N_{qs}$ | 20 |
| Dilation angle, $\psi$ (°) | 8.5 |
| Effective unit weight, $\gamma_s'$ (kN/m3) | 10 |
| Fluke tip bearing factor, $N_t$ | 0.1 |
| Surface undrained shear strength, $s_{u0}$ | 0 |
| Undrained shear strength gradient, | 1.5 |
| Effective clay unit weight, $\gamma_c'$ (kN/m3) | 7.19 |
| Clay bearing capacity factor, $N_c$ | 9 |
| Clay layer depth, $d_c$ (m) | 5.31 |

Figure 3 shows a perfect agreement between the developed spreadsheet and the existing experimental and analytical studies.

### 3.3 Anchors Selected for Reliability Studies

Stevpris Mk5 and Mk6 were used for reliability analysis in the current study. These anchors are widely used for permanent and temporary station keeping of floating systems. Also, selection of these anchors enabled effective comparison of the reliability results with earlier studies conducted in homogenous clay and sand (Moharrami and Shiri (2018) and Aslkhalili et al. (2019)). The ratio of fluke length to fluke thickness ($L_f/d_f$) in these anchors are 6.67 and 3.09 for Mk5 and Mk6, respectively. The plan and side view and geometrical properties of these anchors could be found in Vryhof Anchors (2010).

## 4 Finite Element Mooring Analysis

A generic semi-submersible platform in the Flemish Pass Basin, Newfoundland offshore was considered with a catenary spread mooring consisting of eight mooring legs. Each line includes three segments; the upper, middle, and lower part which are made up of chain, wire rope, and chain, respectively. The dynamic line tensions at the touchdown point (TDP) were obtained using a finite element model developed in Orca Flex. Performing a three hours time-domain simulation revealed that the environmental loads with a 100 years return period (i.e., $H_s$ = 9.5 m, $T_P$ = 12.8 s, and $U_{10}$ = 29 m/s) results in the most heavily loaded line which is in agreement with DNV-RP-F109 (2010) recommendation. The incorporated response amplitude operator (RAO) of the platform for the head sea indicated in Figure 4.

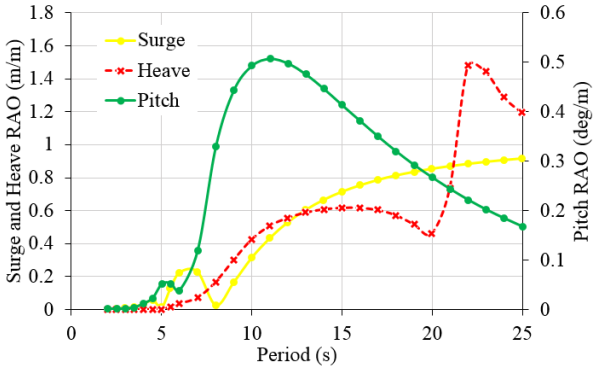


Figure 4. Generic semisubmersible RAO, the head sea

Table shows the primary outcome of dynamic mooring analysis including $T_d$ (design line tension), $\theta_o$ (line angle at mudline), $T_{mean\text{-}C}$ (characteristic mean tension), and $T_{dyn,max\text{-}C}$ (characteristic mean maximum dynamic tension). These results were used in reliability analysis.

Table 2. Characteristic of the catenary mooring system

| $H_s$ (m) | $T_P$ (s) | $U_{10}$ (m/s) | $T_{mean\text{-}C}$ (kN) | $T_{dyn,max\text{-}C}$ (kN) | $T_d$ (kN) | $\theta_o$ (°) |
|---|---|---|---|---|---|---|
| **9.5** | 12.8 | 29 | 846 | 623 | 2493 | 1.3 |

## 5 Reliability Analysis

First order reliability method (FORM) was used through an iterative technique to get the probabilistic results by consideration of uncertainties in the seabed properties and environmental loads. The limit equilibrium method proposed by O'Neill et al. (1997) was adopted for probabilistic modeling of the anchor capacity in layered soil (clay over sand). The embedment trajectory and the chain frictional capacity were accounted in the ultimate holding capacity calculations. The uncertainties related with environmental loads and metocean variables like wind velocity, spectral peak period, significant wave height, and consequently the stress distribution throughout the catenary lines were considered by defining appropriate probability density function and the response surface approach. Based on recommendations of DNV-RP-E301 (2012), a target failure probability and consequence class of 10E-5 and 2 were set in this study.

### 5.1 Limit State Function

The anchor holding capacity and the mooring line tensions at mudline were used to construct the limit state function (DNV-RP-E301 2012):

$$M = R_d - T_d \quad [3]$$

where $T_d$ and $R_d$ are the design line tension and design anchor and chain system capacity at mudline, respectively. The design line tension, $T_d$, was formulated as the sum of the characteristic mean line tension, $T_{mean\text{-}C}$, and the characteristic dynamic line tension, $T_{dyn,max\text{-}C}$. The characteristic mean line tension, $T_{mean\text{-}C}$, is the result of the line pretension and mean environmental loads. The maximum dynamic line tension, $T_{dyn,max\text{-}C}$, is representing the low-frequency and wave-frequency vessel motions. Based on DNV-RP-E301 (2012) recommendations, the dynamic and characteristic mean line tensions were multiplied by relevant partial safety factors, $\gamma_{dyn}$ and $\gamma_{mean}$, respectively.

$$T_d = T_{mean-C} \cdot \gamma_{mean} + T_{dyn-C} \cdot \gamma_{dyn} \quad [4]$$

The partial safety factors for mean and dynamic line tension was taken as 1.4 and 2.1 for consequence class 2 (DNV-RP-E301 2012). The significant wave height ($H_s$), peak period ($T_p$), and wind velocity ($U_{10}$) were used as primary parameters of the extreme sea-state. Both $T_{mean\text{-}C}$ and $T_{dyn,max\text{-}C}$ were expressed as a function of those parameters at the mudline; therefore, the limit state function can be written as:

$$M(R, H_s, T_p, U_{10}) = R_d - T_{mean-C}\,\gamma_{mean} - T_{dyn,max-C}\,\gamma_{dyn} \quad [5]$$

The failure probability $p_F$ for a given extreme sea state was defined as:

$$p_F = P[M(R, H_s, T_p, U_{10}) \leq 0] \quad [6]$$

The annual probability of failure ($p_{Fa}$) for the incidence of extreme sea states was defined by adopting a Poisson model and using an exponential function of failure probability ($p_F$) (Silva-González et al. 2013):

$$p_{Fa} = 1 - exp(-\lambda p_F) \quad [7]$$

where λ indicates the number of occurred extreme sea states throughout the observation period in years.

## 5.2 Probabilistic Modelling of Anchor Capacity

The anchor capacity database in layered seabed (clay over sand) was constructed by using the key anchor-seabed interaction factors including undrained shear strength ($s_{ug}$), the side shear factor ($\alpha_s$), effective clay and sand weight ($\gamma'_c$, $\gamma'_s$), fluke bearing factor ($N_c$), sand friction angle ($\phi_p$), and dilation angle ($\psi$). For homogeneous clay domain, the same properties used by Moharrami and Shiri (2018) were adopted to be able to perform a comparative study. A lognormal distribution with mean value ($\mu s_{ug}$) of 1.5 kPa/m and a coefficient of variation ($\delta s_{ug}$) of 0.2 was used for undrained shear strength. A bivariate lognormal distribution was used for fluke bearing and side friction factors with a mean values $\mu_{\alpha s}$ of 0.7 and $\mu_{Nc}$ of 9. A coefficient of variation $\delta_{\alpha s}$ equal to 0.2 and $\delta_{Nc}$ of 0.25 was used with a correlation coefficient of -0.8, (ρ). The effective clay weight was considered by using a normal distribution with a mean value ($\mu_{\gamma'_c}$) of 7.19 and a coefficient variance ($\delta_{\gamma'_c}$) of 0.07 (Phoon and Kulhawy 1999). For the homogeneous sand layer, the same magnitudes suggested by Aslkhalili et al. (2019) were used to be able to have a comparative study. A lognormal distribution was set for peak friction angle with the mean ($\mu_{\phi_p}$) and coefficient of variation ($\delta_{\phi_p}$) equal to 35° and 0.05, respectively. For dilation and sand unit weight, a normal distribution was adopted with the following properties. The mean value for soil density ($\mu_{\gamma'_s}$) and the related coefficient variance ($\delta_{\gamma'_s}$) were taken as 10.07 and 0.02, respectively. The magnitude of these parameters for dilation angle ($\mu_\psi$ and $\delta_\psi$) were set to 8.49° and 0.28. The database for holding capacity of anchor in layered soil was constructed by performing 8750 simulations and using different values for $s_{ug}$, $\alpha_s$, $\gamma'_c$, $\gamma'_s$, $N_c$, $\phi_p$, $\psi$. In order to investigate the effect of clay layer depth on holding capacity of anchor, two different clay layer depths ($d_c$) of 1.07$L_f$ and 1.39$L_f$ were studied.

Figure 5. shows the curve fits for distribution and the histograms of the anchor capacities at mudline for Mk5 with $L_f$ = 4.297 in layered soil ($d_c$ = 1.39$L_f$).

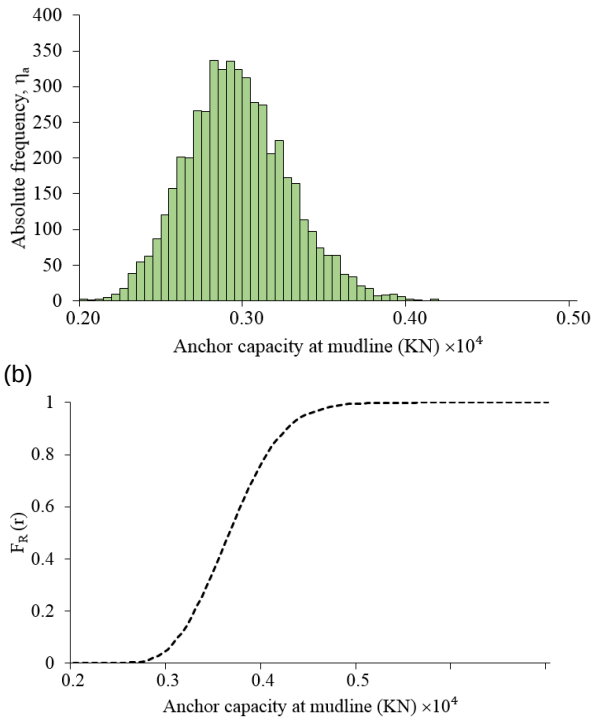


Figure 5. Histograms of simulated capacities at mudline, (a) absolute frequency, (b) cumulative frequency

5.3 Probabilistic Model of Line Tension

To develop the response surfaces an approach proposed by Silva-González et al. (2013) was adopted. The dynamic line tensions were defined by using a Gaussian process (Choi, 2007; Sarkar and Eatock Taylor, 2000) by expressing its maximum magnitude during an extreme sea state using the model proposed by Davenport (1964). The extreme sea state (Θ) was represented by using a random vector of r uncertain environmental variables:

$$\mathrm{E}\left[T_{dyn,max}\right]_{\Theta} = \mu_{Tdyn,max}\left[\sqrt{2\ln\left(\nu_{\Theta}\Delta t/2\right)} + \frac{0.5772}{\sqrt{2\ln\left(\nu_{\Theta}\Delta t/2\right)}}\right]\sigma_{T,\Theta} \quad [8]$$

where, $\Delta t$ is the duration of extreme sea state; $\sigma_{T,\Theta}$ (or $\sigma(\Theta)$) is the standard deviation; and $\nu_{\Theta}$ (or $\nu(\Theta)$) is the mean crossing rate of the dynamic line tension. The predicted maximum dynamic line tension at mudline ($T_{dyn,max}$) and the mean line tension ($T_{mean}$) were formulated using a second order polynomial expansion in terms of Θ:

$$Y(\Theta) = c + a^{T}\Theta + \Theta^{T}b\Theta \quad [9]$$

where Θ and Y(Θ) are the r × 1 vector of environmental variables and the response of interest, respectively. Response analysis was adopted to determine the subsequent unknown coefficients c, a (r ×1), and b (r ×r). The response surfaces were developed by using seven critical environmental parameters obtained from the mooring system in the Flemish Pass Basin located in East Newfoundland offshore region. A database comprised of 8100 different combinations of environmental variables was constructed by using of differing environmental variables including significant wave height ($H_s$), direction of wave ($d_w$), peak period ($T_p$), velocity of wind ($U_{10}$), direction of wind ($d_{ww}$), speed of surface current ($U_c$), and current direction relative to wave direction ($d_{wc}$). The mooring line going under the highest load was investigated to get the response surface.

A storm event was used to identify the extreme sea states. A time window was defined around the peak period by using clustering and de-clustering ($t_{peak}$ - $\Delta T_{cluster}$, $t_{peak}$ - $\Delta T_{cluster}$). The extreme sea state occurs if a significant wave height is reached at tpeak which is higher than the threshold amount (Hs ≥ Hsth). The other environmental variables were determined based on the peak period (tpeak). The marginal probability distribution of Θ (or [Hs, Tp, U10]$^{T}$) was generated by using the peaks over threshold approach and a set of 24 extreme sea states within the hindcast time series. The amount of mean annual rate λ is 1.25, (30/24), per year according to the maximum probability estimate. Table and 4 summarize the best fitted marginal distributions, the parameters related to maximum likelihood estimate, and correlation coefficients for main environmental variables.

Table 3. Distribution parameters of environmental variables

| Variable | Probability distribution | Distribution parameters | |
|---|---|---|---|
| $\mathbf{H_s}$ | Weibull | Scale | 9.5351 |
| | | Shape | 10.1552 |
| $\mathbf{T_p}$ | Lognormal | $\mu_{\ln T_p}$ | 2.4966 |
| | | $\sigma_{\ln T_p}$ | 0.1196 |
| $\mathbf{U_{10}}$ | Lognormal | $\mu_{\ln U_{10}}$ | 3.4827 |
| | | $\sigma_{\ln U_{10}}$ | 0.1095 |

Table 4. Estimated correlation coefficients

| | $\mathbf{H_s}$ | $\mathbf{T_p}$ | $\mathbf{U_{10}}$ |
|---|---|---|---|
| $\mathbf{H_s}$ | 1.0 | 0.9728 | 0.9905 |
| $\mathbf{T_p}$ | 0.9728 | 1.0 | 0.9935 |
| $\mathbf{U_{10}}$ | 0.9905 | 0.9935 | 1.0 |

5.4 Results of Reliability Analysis

Figure 6. illustrates the variation of annual reliability index versus fluke length (plot a) and dry anchor weight (plot b) in two different clay layer depth (1.07$L_f$, 1.39$L_f$). Each point on plot A linked to an equivalent point on plot B and vice versa. As shown in
Figure 6., at any clay depth, different anchor families with different weight and fluke lengths could be used to reach a specified reliability target. For achieving target failure probabilities between 10-4 and 10-5 (with $d_c$=1.39$L_f$), the existing weight and fluke length for MK5 is 22 t and 4.436 m and for MK6 is 18 t and 4.534 m. The mentioned target failure probabilities are generally used as the ultimate limit state design in offshore systems (DNV-OS-E-301 2010; DNV-OS-F201, 2010; DNV-OS-F101, 2013). Also, at a given clay layer depth, two different anchor families with the same weight and different fluke length result in different annual reliability indexes. Similar to homogeneous clay condition (Moharrami and Shiri 2018), the capacity of deeply embedded anchors in layered soil (clay over sand) is significantly affected by fluke length, while the anchor weight is not a significant factor. In each anchor family, the annual reliability index increases when the clay layer depth increases. The logarithmic variation of failure probability (log ($P_{Fa}$)) against anchor weight and fluke length with their linear curve fit in two different clay layer depth ($d_c$) for MK5 and MK6 anchor families are shown in Figure 7. The required increment of anchor fluke length and weight to decrease the annual failure probability for one order of magnitude (by a factor of 10) could be achieved by finding the slope of each curve. These outcomes are useful in the life cycle cost-benefit analysis, where finding the initial cost model as a function of the failure probability is required.
a)

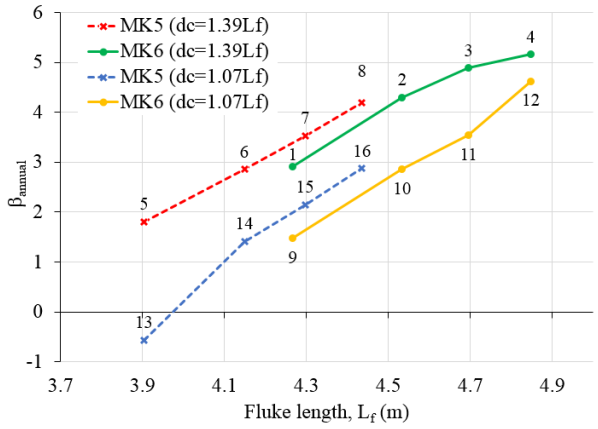


b)

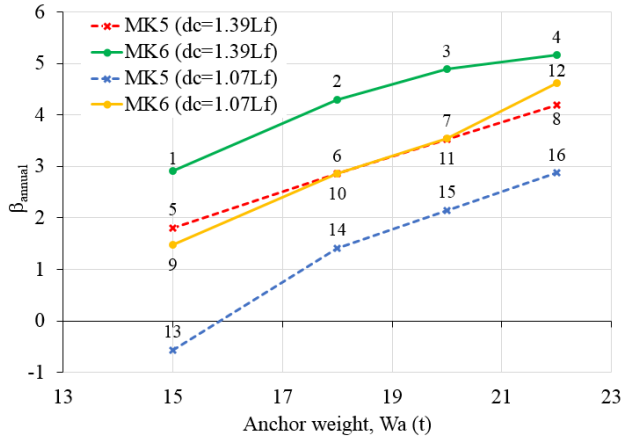


Figure 6. Annual reliability index versus (a) fluke length, and (b) anchor weight

By increasing the weight and fluke length of the anchor, which are associated with the mass and volume of the anchor, the initial cost and failure probability will increase and decrease respectively. Figure 7 shows that in each clay layer depth ($d_c$=1.07$L_f$ and $d_c$=1.39$L_f$) the slope of the MK6 anchor family is higher than the MK5 family. Therefore, a small deviation in fluke weight and fluke length causes considerable variation in failure probability and reliability index.

a)

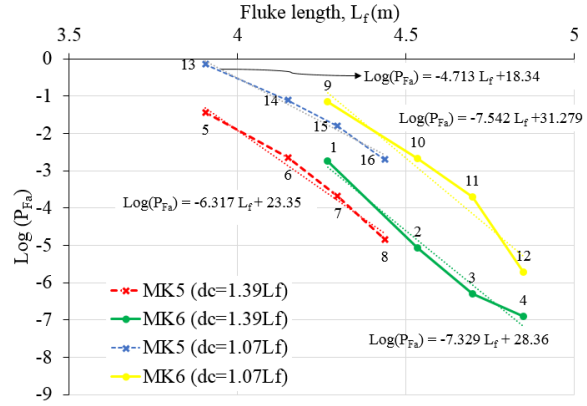


(b)

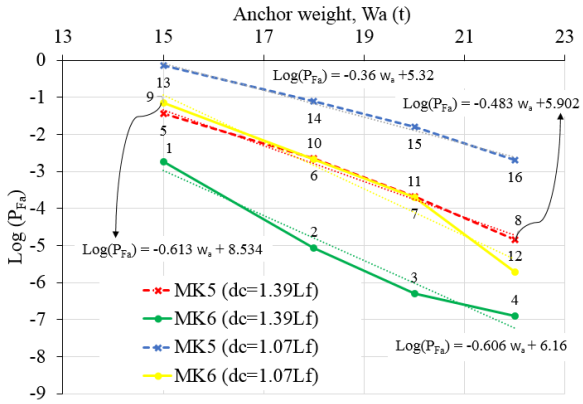


Figure 7. The logarithm of failure probability versus (a) fluke length, and (b) anchor weight

## 5.5 Comparison between the reliability of anchors in homogenous and layered Soils

The results of reliability assessment in layered soil (clay over sand) were compared with the earlier reliability investigation in the homogenous soil; clay (Moharrami and Shiri 2018) and sand (Aslkhalili et al. 2019). This was facilitated by selecting the same properties of homogenous clay and sand layers from the aforementioned studies to define the soil layers in layered stratum (clay over sand). Figure 8. shows the variation of annular reliability index versus anchor weight in sand, clay, and, clay over sand for MK5 and MK6, with clay layer depths of 1.07$L_f$ and 1.39$L_f$.

(a)

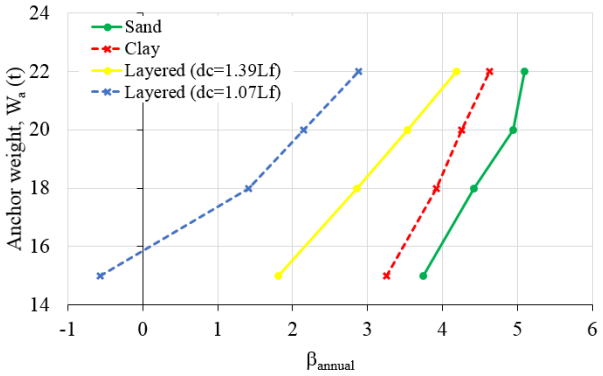


(b)

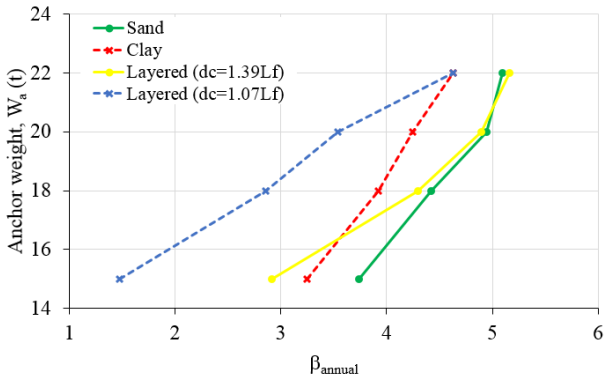


Figure 8. Annular reliability index versus anchor weight (a) MK5, (b) MK6

## 6 Conclusion

The primary outcomes of the study are summarized as follow:

The seabed soil stratum and its configuration (individual layer thickness) have a significant influence on reliability indexes. Overall, the probability of failure is higher for the layered clay over sand stratum compared with homogeneous clay and sand layers.

The geometrical anchor configuration, particularly the fluke length, was found to have a significant effect on holding capacity and consequently the reliability indexes. The geometrical improvement of the anchors can effectively improve their reliability. In addition, the current design practice is identical for all of the different anchor families. This approach does not account for the significant influence of anchor geometry and the uncertainties associated with different anchor families, environmental, and operational loads. The reliability-based refinement of the design procedure can considerably improve the reliability and cost-effectiveness of anchor design.

The configuration of layered soil strata, particularly the depth and thickness of layers showed a significant effect on ultimate holding capacity and reliability indexes. Thicker clay layers resulted in higher reliability indexes. Different range of layer thickness still needs to be investigated to generalize the obtained results.

The current study was limited to specific anchor families performing in clay over sand seabed strata with two instances of layer thickness. Further investigations are necessary for different layer configurations and different anchor families.


### Acknowledgments

The authors gratefully acknowledge the financial support of this research by Memorial University of Newfoundland through VP start-up fund and school of graduate studies (SGS). The technical advice of Mr. Mohammad Javad Moharrami and Mr. Rahim Shoughi is also kindly acknowledged.


### References


Aslkhalili, A., Shiri, H., and Zendehboudi, S. 2019. Reliability assessment of drag embedment anchors in sand and the effect of idealized anchor geometry. Safety in Extreme Environments, 1(1–3): 39–57. Safety in Extreme Environments. doi:10.1007/s42797-019-00006-5.

Choi, Y.J. 2007. Reliability Assessment of Foundations for Offshore Mooring Systems under Extreme Environments.

Clukey, E.C., Gilbert, R.B., Andersen, K.H., and Dahlberg, R. 2013. Reliability of Suction Caissons for Deep Water Floating Facilities. 1991(2005): 456–474. doi:10.1061/9780784412763.035.

Davenport, A.G. 1964. Note on the Distribution of the Largest Value of a Random Function With Application To Gust Loading. Proceedings of the Institution of Civil Engineers, 28(2): 187–196. doi:10.1680/iicep.1964.10112.

DNV-OS-E-301. 2010. Position Mooring. Offshore Standard.

DNV-OS-F101. 2013. Submarine Pipeline Systems. Offshore standartd.

DNV-OS-F201. 2010. Dynamic Risers. Offshore Standard.

DNV-RP-E301. 2012. Design and Installation of Fluke Anchors.

DNV-RP-F109. 2010. On-bottom stability design of submarine pipelines.

Duggal, A., Ma, K., Shu, H., Smedley, P., and L'Hostis, D. 2013. A Historical Review on Integrity Issues of Permanent Mooring Systems. **3**. doi:10.4043/24025-ms.

Moharrami, M.J., and Shiri, H. 2018. Reliability assessment of drag embedment anchors in clay for catenary mooring systems. Marine Structures, **58**(November 2017): 342–360. Elsevier Ltd. doi:10.1016/j.marstruc.2017.12.005.

Montes-Iturrizaga, R., and Heredia-Zavoni, E. 2016. Reliability analysis of mooring lines using copulas to model statistical dependence of environmental variables. Applied Ocean Research, 59: 564–576. Elsevier B.V. doi:10.1016/j.apor.2016.07.008.

Neubecker, S.R., and Randolph, M.F. 1996a. The kinematic behaviour of drag anchors in sand. Canadian Geotechnical Journal, **33**(4): 584–594. doi:https://doi.org/10.1139/t96-084-306.

Neubecker, S.R., and Randolph, M.F. 1996b. The static equilibrium of drag anchors in sand. Canadian Geotechnical Journal, **33**(4): 574–583.

O'Neill, M.P. 2000. The behaviour of drag anchors in layered soils, PhD Thesis, Department of Civil Engineering, The University of Western Australia.

O'Neill, M.P., Randolph, M.F., and House, A.R. 1997. A preliminary assessment of the behaviour of drag anchors in layered soils. 9(November).

Phoon, K.K., and Kulhawy, F.H. 1999. Characterization of geotechnical variability. Canadian Geotechnical Journal, 624: 612–624.

Rendón-Conde, C., and Heredia-Zavoni, E. 2016. Reliability analysis of suction caissons for moored structures under parameter uncertainties. Structural Safety, 60: 102–116. doi:10.1016/j.strusafe.2016.02.004.

Sarkar, A., and Eatock Taylor, R. 2000. Effects of mooring line drag damping on response statistics of vessels excited by first- and second-order wave forces. Ocean Engineering, 27(6): 667–686. doi:10.1016/S0029-8018(99)00014-1.

Silva-González, F., Heredia-Zavoni, E., Valle-Molina, C., Sánchez-Moreno, J., and Gilbert, R.B. 2013. Reliabilitystudy of suction caissons for catenary and taut-leg mooring systems. Structural Safety, 45: 59–70. Elsevier Ltd. doi:10.1016/j.strusafe.2013.08.011.

Valle-molina, C., Heredia-zavoni, E., and Silva-gonzález, F.L. 2008. Reliability analyses of suction caissons for FPSO systems. *In* International Conference on Offshore Mechanics and Arctic Engineering. pp. 1–6.

Vryhof Anchors. 2010. Anchor manual. Krimpen ad Yssel, The Netherlands.